arXiv:1304.7469v1 [quant-ph] 28 Apr 2013

Asking photons where have they been

A. Danan, D. Farfurnik, S. Bar-Ad, and L. Vaidman

Raymond and Beverly Sackler School of Physics and Astronomy
Tel-Aviv University, Tel-Aviv 69978, Israel

Quantum mechanics does not provide a clear answer to the question: What was the past of a photon which went through an interferometer [1]? Various *welcher weg* measurements [2], delayed-choice which-path experiments [3–5] and weak-measurements of photons in interferometers [6–8] presented the past of a photon as a trajectory or a set of trajectories. We have carried out experimental weak measurements of the paths of photons going through a nested Mach-Zehnder interferometer, discussed earlier in another context [9, 10] which show a different picture: the past of a photon is not a set of continuous trajectories. The photons tell us that they have been in the parts of the interferometer which they could not have possibly reached! Our results lead to rejection of a "common sense" approach to the past of a quantum particle. On the other hand they have a simple explanation within the framework of the two-state vector formalism of quantum theory [11, 12].

The idea is simple, and analogous to the following scenario: If our radio plays Bach, we know that the photons come from a classical music station, but if we hear a traffic report, we know that the photons come from a local radio station. We can deduce where the photons were on the basis of the information they provide.

In our experiment we vibrate various mirrors inside the interferometer at different frequencies. The rotation of a mirror causes a vertical shift of the light beam reflected off that mirror. We measure the position of photons coming out of the interferometer, and Fourier-analyze the output signal. When the vibration frequency of a certain mirror appears in the power spectrum, we conclude that photons have been near that particular mirror. The vertical displacement of the beam due to the rotation of the mirrors is significantly smaller than the width of the beam, and the change in the optical path length is much smaller than the wavelength. This ensures that the disruption of the interference in the experiment is negligible.

We start with a Mach-Zehnder interferometer (MZI) aligned in such a way that every photon ends up in detector D, see Fig. 1A. Mirrors A and B vibrate around their horizontal axes at frequencies f_A and f_B respectively, causing an oscillation of the vertical position of the photons reaching the detector. The detector D is a quad-cell photo-detector, and the measured signal is the difference of the currents generated in its upper and lower cells. Experimental details are described in the Supplementary information. As expected, the power spectrum shows two equal contributions at frequencies f_A and f_B.

This observation does not answer the question: Did each photon pass through a single arm or through both arms of the interferometer? While the quantum wave of the photon passed through both arms, our measurement does not prove it. The observed current was created by numerous photons, so conceivably different ones were responsible for the two peaks of the power spectrum. Nevertheless, the measurements provide a conclusive evidence that at least some of the observed photons passed near mirrors A and B.

We also measure the signal from the detector when the second beam splitter is removed, transforming the experiment to a which-path measurement, Fig. 1B. Only the signal with frequency f_B remains.

Next, we build a larger interferometer, Fig. 2A, in which one third of the beam power goes to

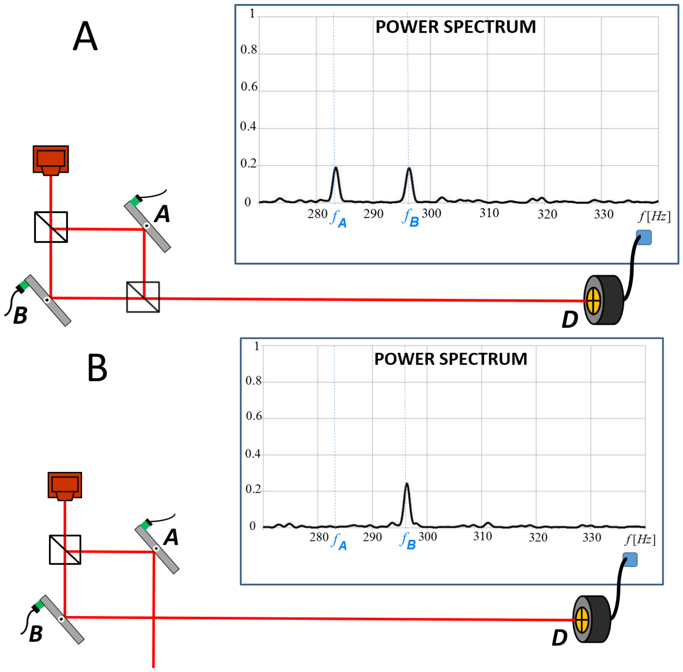

FIG. 1: (A) Measured power spectrum of the signal from the quad-cell photo-detector shows frequencies of oscillation of internal mirrors A and B of the Mach-Zehnder interferometer. (B) Only the frequency of the mirror B remains in the power spectrum of the signal when the second beam splitter of the interferometer is taken out.

the lower arm and two thirds of the beam power pass through the interferometer we just described, in the upper arm. We align the inner (nested) interferometer and the large interferometer in such a way, that again all the photons end up in detector D. We vibrate all the mirrors around their horizontal axes with equal (small) amplitudes, each at a different frequency. As expected, the power spectrum shows peaks at all frequencies, and the peaks at frequencies f_E and f_F are higher than the rest.

The surprising result is obtained when the interferometer is modified to be a which-path experiment, using the nested MZI as a switch. By slightly shifting mirror B we align the MZI so that there is complete destructive interference of the light propagating towards mirror F, see Fig. 2B. In that case observing photons at D supposedly implies that those photons chose the lower arm of the interferometer. We thus expect that the photons reaching detector D have interacted only with mirror C, and that the measured signal should therefore show only the frequency f_C. Yet the results of the experiment are different: we observe *three* peaks of approximately the same strength: the expected one at frequency f_C, and two more peaks at frequencies f_A and f_B. The photons tell us that they also interacted with the mirrors of the nested interferometer in the upper arm! To verify the destructive interference of the light directed towards mirror F we blocked the lower arm, see Fig. 2C. The result was a null signal with no peaks at all.

A particulary surprising feature of the power spectrum of Fig. 2B is the presence of peaks at f_A and f_B and the absence of peaks at f_E and f_F. The photons passing through the inner interferometer have to be reflected off the mirrors E and F and thus they are expected to yield even higher peaks at frequencies f_E and f_F.

Our interference experiments utilizes visible light with about 10^{14} photons at each run. Thus, even Maxwell's equations for the classical electromagnetic field should explain the observed phe-

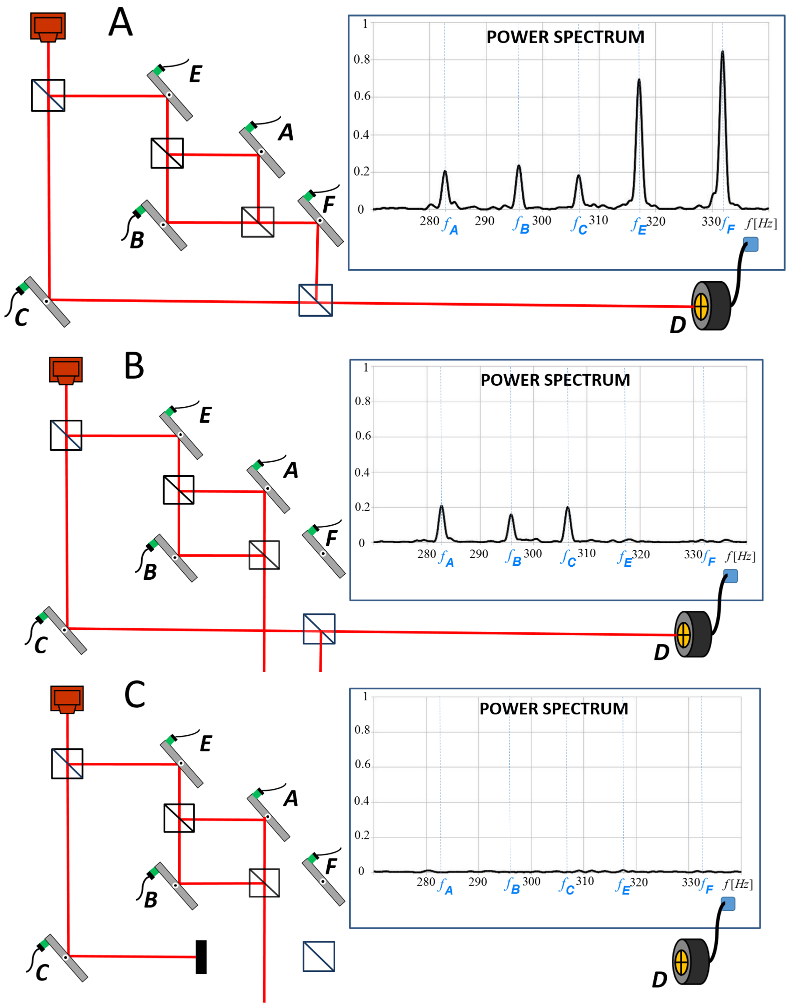

FIG. 2: (A) Measured power spectrum of the signal from the quad-cell photo detector shows frequencies of oscillation of all internal mirrors of the interferometer. (B) When the inner interferometer is tuned in such a way that the beam of light passing through it does not reach the photo-detector, the power spectrum of the signal in the photo-detector still shows frequencies of the mirrors of this interferometer. (C) These frequencies (and all other signals) disappear when we, without changing anything in the upper arm, block the lower arm of the large interferometer.

nomena. Yet how can these results be explained without encountering the paradoxical feature of the light carrying information about mirrors near which it has not been? The clue is the tiny leakage of light in the inner interferometer (less than 1% in our experiment). However, questions remain: How a tiny amplitude of the wave is, on one hand, practically invisible when C is blocked (Fig. 2C) and at the same time causes an effect of the same order as the effect of mirror C, through which most of the wave passes, when the latter is not blocked? Why the oscillations of mirrors E and F, from which the upper arm wave is reflected, do not show up at all?

As we will show below, the formal answers to these questions can be given through calculation of the interference of the electromagnetic field. The calculations are simple, but the picture of evolving electromagnetic wave does not provide an intuition that could tell us beforehand that this will be the result. The intuitive picture which allows to foresee these results is given by the two-state vector formulation (TSVF) of quantum mechanics [11, 12]. The observed behavior applies equally

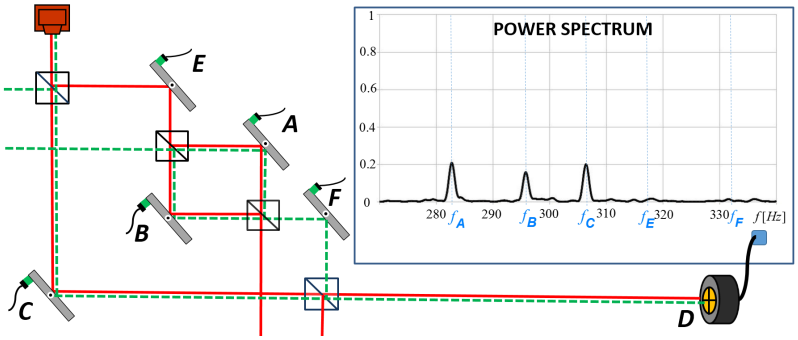

FIG. 3: The two-state vector description of the photon inside the interferometer includes the standard forward evolving quantum state (red line) and backward evolving quantum state (green dashed line) of the photon detected by the quad-cell photo-detector. It provides an explanation of the observed power spectrum: frequencies f_C, f_A and f_B are present while f_E and f_F are not. The photon was present only where both forward and backward quantum wave functions do not vanish.

if the experiment is performed with single photons [13] or with a macroscopic number of photons. In the TSVF each photon observed by detector D is described by the backward-evolving quantum state $\langle\Phi|$ created at the detector, in addition to the standard, forward-evolving wave function $|\Psi\rangle$ created at the source. The equations of the TSVF imply that a photon can have a local observable effect only if both the forward- *and* backward-evolving quantum waves are non-vanishing at this location. Fig. 3. shows the forward and the backward evolving states inside the interferometer in the setup of Fig. 2B. It does explain the peculiar features of the power spectrum. The peaks at frequencies f_A, f_B, and f_C correspond to the fact that near mirrors A, B, and C both forward evolving and backward evolving quantum states are present. The absence of the peak at f_E follows from the absence of the backward evolving wave near E while the absence of the forward evolving wave near F explains why we do not see a peak at f_F. It is a simple exercise to show that the same argument explains the power spectrum in all the other examples presented above.

Let us describe the experiment in the framework of the TSVF in more detail. The two-state vector of the photon at the moment that its partial wave packets bounce off the mirrors A, B and C is

$$\langle\Phi|\ |\Psi\rangle = \frac{1}{\sqrt{3}}\left(\langle A| - \langle B| + \langle C|\right)\quad \frac{1}{\sqrt{3}}\left(|A\rangle + |B\rangle + |C\rangle\right), \tag{1}$$

where we used natural notation: $|A\rangle$ is a localized wave packet near mirror A, etc. (Note that the same two state vector describes the particle in the so called "Three-box paradox" [14].)

The main result of the TSVF is that any weak enough coupling to a variable O of a pre- and post-selected system results in an effective coupling to the *weak value* of O:

$$O_w \equiv \frac{\langle\Phi|O|\Psi\rangle}{\langle\Phi|\Psi\rangle}. \tag{2}$$

The rotation of a mirror makes the photon itself the measuring device of its projection operator on the location of the mirror. Since the amplitude of the vibration of the mirrors is $\sim 1.3\cdot 10^{-7} rad$ while the quantum uncertainty of the direction of the photon is $\sim 3.7\cdot 10^{-4} rad$, this is a *weak measurement* of the projection. The pointer variable is the transverse momentum of the photon which is transformed to a spatial shift at the detector. Using (1) and (2) we calculate the weak values of the projection operators at mirrors A, B and C: $(\mathbf{P}_A)_w = (\mathbf{P}_C)_w = 1$, $(\mathbf{P}_B)_w = -1$. Obviously, $(\mathbf{P}_E)_w = (\mathbf{P}_F)_w = 0$. This explains the equal peaks at frequencies f_A, f_B, and f_C and the absence of peaks at f_E and at f_F in Fig. 3B. The peak at f_B is the same as at f_A and f_C because the power spectrum shows only the size of the signal, not its sign.

The TSVF adds no new predictions beyond standard quantum mechanics. It just provides a simple intuitive picture of pre- and post-selected quantum systems. In the standard framework of quantum mechanics it is not easy to foresee these effects, but when the question is asked, the calculation is simple. Essentially, the same explanation holds also for a classical electromagnetic wave. Let us describe the electromagnetic field of the wave reaching our quad-cell detector as a function of y: the difference of the integrals of the intensity over the regions $y > 0$ and $y < 0$ is our signal. We consider the setup described on Fig. 2B and assume that only mirror C is rotated by a small angle. The wave reaching the quad-cell detector can be viewed as a superposition of three Gaussian type waves of equal weight bounced off mirrors A, B, and C, which, up to normalization, are $\Psi_C = e^{-\frac{(y-\delta)^2}{2a^2}}$, $\Psi_A = e^{-\frac{y^2}{2a^2}}$, and $\Psi_B = -e^{-\frac{y^2}{2a^2}}$. Their superposition is just $e^{-\frac{(y-\delta)^2}{2a^2}}$, the Gaussian shifted by δ. This explains the peak around f_C. But if instead of rotating mirror C, we rotate in the same way mirror A, the result will be exactly the same! This explains the peak at f_A. If, instead, we rotate mirror B, the result will not be exactly the same, but for $\delta \ll a$, which is a requirement of our weak measurement, the wave will again be approximately a shifted Gaussian, with a shift $-\delta$. This explains the peak of the same size at f_B. When the lower arm is blocked, Fig. 2C, we obtain a superposition of only Ψ_A, and Ψ_B. The (theoretical) intensity of the total light reaching the quad-cell detector is then smaller by a factor of $\frac{\delta^2}{4a^2} \sim 2.7 \cdot 10^-8$. In practice, due to imperfect alignment, the actual reduction was only by the factor of $\sim 8.0 \cdot 10^-3$. This explains why the vibrations of the mirrors do not result in an observable change of the interference and why a null signal is obtained in this case.

It will be of interest to repeat this experiment in a regime where neither a classical wave evolution description nor a single particle quantum wave description can provide an explanation. One challenging proposal is to perform the same interference experiment with neutrons. A conceptually different approach aiming to find out where were the particles inside an interferometer would be a weak measurement using an external measuring device. Kerr media provide an interaction between photons, and a weak measurement of a projection operator of a single photon is considered feasible [15] for amplified weak values, which, however, is not the case in our setup. Another proposal is to use “a two-photon entangling operation, and post-selection” [16].

In conclusion, we have performed direct measurements which shed new light on the question: Where were the photons passing through an interferometer? The main results are presented in Fig. 2B. The photons themselves tell us where they have been. And the story they tell is surprising. The photons do not always follow continuous trajectories. Some of them have been inside the nested interferometer (otherwise they could not have known the frequencies f_A, f_B), but they never entered and never left the nested interferometer, since otherwise they could not avoid the imprints of frequencies f_E and f_F of mirrors E and F leading photons into and out of the interferometer. The results contradict a naïve approach attributing continuous trajectories to the photons. Only the description with both forward and backward evolving quantum states provides a simple and intuitive picture of pre- and post-selected quantum particles.

Ackowledgements. This work has been supported in part by the Binational Science Foundation Grant No. 32/08, the Israel Science Foundation Grant No. 1125/10 and Sackler Institute of Condense Matter Equipment Grant.

---

[1] L. Vaidman, Past of a quantum particle, *Phys. Rev. A*, to be publsihed (2013).

[2] T. J. Herzog, P. G. Kwiat, H. Weinfurter, and A. Zeilinger, Complementarity and the quantum eraser, *Phys. Rev. Lett.* **75**, 3034 (1995).

[3] V. Jacques, *et al.*, Experimental realization of Wheeler's Delayed-Choice gedanken experiment, *Science* **315**, 966 (2007).

[4] A. Peruzzo, *et al.*, A Quantum Delayed-Choice experiment, *Science* **338**, 634 (2012).

[5] F. Kaiser,*et al.*, Entanglement-Enabled Delayed-Choice experiment, *Science* **338**, 637 (2012).

[6] K.J. Resch, J.S. Lundeen, A.M. Steinberg, Experimental realization of the quantum box problem, *Phys. Lett. A*, **324**, 125 (2004).

[7] S. Kocsis *et al.*, Observing the average trajectories of single photons in a two-slit interferometer, *Science* **223** 1170 (2011).

[8] A. Matzkin, Observing trajectories with weak measurements in quantum systems in the semiclassical regime, *Phys. Rev. Lett.* **109**, 150407 (2012).

[9] O. Hosten *et al.*, Counterfactual quantum computation through quantum interrogation, *Nature* **439**, 949 (2006).

[10] L. Vaidman, Impossibility of the counterfactual computation for all possible outcomes, *Phys. Rev. Lett.* **98**, 160403 (2007).

[11] Y. Aharonov, P. G. Bergmann and J. L. Lebowitz, Time symmetry in the quantum process of measurement, *Phys. Rev. B* **134**, 1410 (1964).

[12] Y. Aharonov and L. Vaidman, Properties of a quantum system during the time interval between two measurements, *Phys. Rev. A* **41**, 11 (1990).

[13] P. Grangier, G. Roger and A. Aspect, Experimental evidence for a photon anticorrelation effect on a beam splitter: A new light on single-photon interferences, *Europhys. Lett.* **1**, 173 (1986).

[14] Y. Aharonov and L. Vaidman, Complete Description of a Quantum System at a Given Time, *J. Phys.* **A 24**, 2315 (1991).

[15] A. Feizpour, X. Xing, and A. M. Steinberg, Amplifying single-photon nonlinearity using weak measurements, *Phys. Rev. Lett.* **107**, 133603 (2011).

[16] G.L. Pryde, J.L. O'Brien, A.G. White, T.C. Ralph, and H.M. Wiseman, Measurement of quantum weak values of photon polarization, *Phys. Rev. Lett.* **94**, 220405 (2005).

Supplementary Information: **Experimental setup**

We describe here experimental details not mentioned in the main text of the paper.

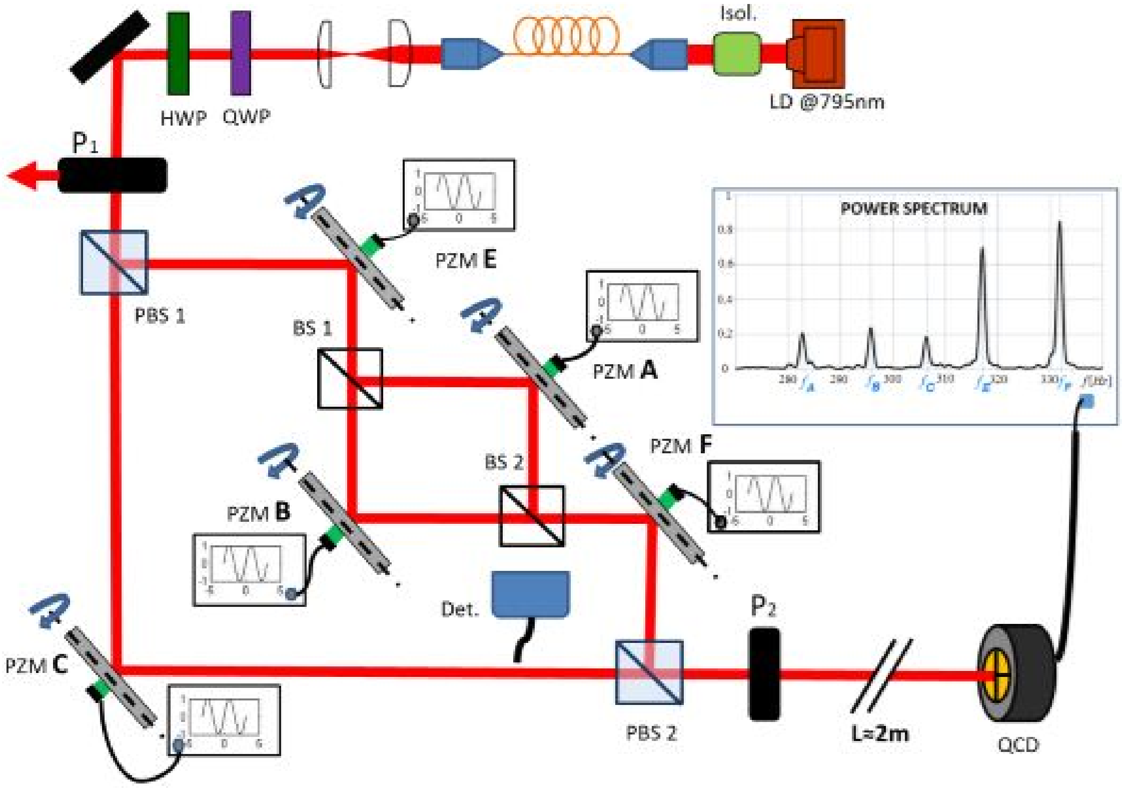

Figure S1: Experimental setup of the nested interferometer – LD- Laser diode; Isol. Faraday isolator; QWP – Quarter wave plate; HWP – Half wave plate; PBS – Polarizing beam splitter; BS – non-polarizing beam splitter; PZM – piezo electric mirror mount; Det. – Photo-detector; P- Glan-Taylor Polarizer; QCD – Quad-cell detector

The inner Mach-Zehnder interferometer (MZI) nested inside the upper branch of the large interferometer is constructed from two non-polarizing beam splitters ($BS_1$and BS_2) and mirrors, Fig. S1. The interference of the nested interferometer is switched from destructive to constructive by translating mirror B and monitoring the output signal at the left port of BS2 using a photo-detector (Det.). The measured interference visibility of the inner MZI is about 98.5%, meaning that only 0.75% of the incoming light exits the dark port. Switching on oscillations of the tilt of the mirrors does not lead to observable change of the interference, but the interference was not stable on the scale of tens of seconds, so we limited each run of the experiment to 1 second during which no significant change of the interference took place.

For the external interferometer, 1:2 beam splitters are implemented utilizing polarizers and polarization beam splitters (not mentioned in a schematic description of the experiment in the text). The input beam is produced using a continuous wave Diode laser ($\lambda \approx 785$nm – Thorlabs-L785P090) as the photon source. A Faraday isolator cancels back reflections, resulting in noise reduction. The beam is spatially filtered and shaped to a ~1mm waist Gaussian beam using a single-mode fiber followed by a beam contraction telescope. The source produced polarized light rotated using quarter-wave and half-wave plates and then filtered by a Glan-Taylor polarizer P_1. The beam splits at a polarization beam splitter PBS_1. This procedure prepares the pre-selected state: $|\Psi\rangle = \sqrt{\frac{1}{3}}|L\rangle + \sqrt{\frac{2}{3}}|\mathrm{U}\rangle$, where $|L\rangle$ and $|U\rangle$ are the lower and upper branches of the external interferometer, respectively.

The lower and upper branches are combined by PBS_2, and then we post-select the final state $|\Phi\rangle = \sqrt{\frac{1}{3}}|L\rangle + \sqrt{\frac{2}{3}}|\mathrm{U}\rangle$, using a polarizer P_2 at angle ~54.7°.

Mirrors A, B, C, E and F are mounted on piezo-electrically-driven mirror mounts (PZMs), and weak sinusoidal modulations of the tilt around horizontal axes are used to introduce vertical shift of the beam reaching the quad-cell photo-detector. Each mirror is seeded with a different sine frequency voltage (~200mmVpp) that resulted in small amplitude oscillation (~300nrad) of the reflected beam. At the output of the interferometer we measured the beam vertical position using a quad-cell photo-detector (QCD, First Sensor QP50-6-SD2) placed at a distance of ~2m from the interferometer. The size of the beam on the detector is ~1.2mm and the displacement caused by the mirrors oscillations is about ±500nm. The QCD signal was sampled using a data acquisition card (NI USB-6008) at a rate of 2.5 KHz during 1 second intervals. We performed a harmonic analysis using MATLAB and created smoothed power spectrum of the signal. The typical results for each interference arrangement are shown in figures 1 and 2.

Note that the quad-cell photo-detector senses photons coming from a wide angle, so backward evolving state of the detected photon is much wider than what is shown on Fig. 3, but this does not change the argument: the backward evolving quantum wave is not reflected off the mirror E.